Control and State Estimation of the One-Phase Stefan Problem via Backstepping Design

Shumon Koga, *Student Member, IEEE,* Mamadou Diagne, *Member, IEEE,* and Miroslav Krstic, *Fellow, IEEE*

***Abstract*—This paper develops a control and estimation design for the one-phase Stefan problem. The Stefan problem represents a liquid-solid phase transition as time evolution of a temperature profile in a liquid-solid material and its moving interface. This physical process is mathematically formulated as a diffusion partial differential equation (PDE) evolving on a time-varying spatial domain described by an ordinary differential equation (ODE). The state-dependency of the moving interface makes the coupled PDE-ODE system a nonlinear and challenging problem. We propose a full-state feedback control law, an observer design, and the associated output feedback control law of both Neumann and Dirichlet boundary actuations via the backstepping method. Also, the state-feedback control law is provided when a Robin boundary input is considered. The designed observer allows estimation of the temperature profile based on the available measurements of liquid phase length and the heat flux at the interface. The associated output feedback controller ensures the global exponential stability of the estimation errors, the $\mathcal{H}_1$-norm of the distributed temperature, and the moving interface at the desired setpoint under some explicitly given restrictions on the setpoint and observer gain.**

***Index Terms*—Stefan problem, backstepping, distributed parameter systems, moving boundary, nonlinear stabilization.**

I. Introduction

a) Background:

STEFAN problem, known as a thermodynamical model of liquid-solid phase transition, has been widely studied since Jeseph Stefan's work in 1889 [39]. Typical applications include sea ice melting and freezing [27], [42], continuous casting of steel [31], crystal-growth [9], thermal energy storage systems [43], and lithium-ion batteries [38]. For instance, time evolution of the Arctic sea ice thickness and temperature profile was modeled in [27] using the Stefan problem, and the correspondence with the empirical data was investigated. Apart from the thermodynamical model, the Stefan problem has been employed to model population dynamics that describes tumor growth process [13] and information diffusion on social networks [25].

While phase change phenomena described by the Stefan condition appear in various kinds of science and engineering processes, their mathematical analysis remains quite challenging due to the implicitly given moving interface that reflects the time evolution of a spatial domain, so-called "free boundary problem" [14]. Physically, the classical one-phase Stefan problem describes the temperature profile along a liquid-solid material, where the dynamics of the liquid-solid interface is influenced by the heat flux induced by melting or solidification phenomena. Mathematically, the problem involves a diffusion partial differential equation (PDE) coupled with an ordinary differential equation (ODE). Here, the PDE describes the heat diffusion that provokes melting or solidification of a given material and the ODE delineates the time-evolution of the moving front at the liquid-solid interface.

While the numerical analysis of the one-phase Stefan problem is broadly covered in the literature, their control related problems have been addressed relatively fewer. In addition to it, most of the proposed control approaches are based on finite-dimensional approximations with the assumption of an explicitly given moving boundary dynamics [10], [1], [30]. Diffusion-reaction processes with an explicitly known moving boundary dynamics are investigated in [1] based on the concept of inertial manifold [7] and the partitioning of the infinite dimensional dynamics into slow and fast finite dimensional modes. Motion planning boundary control has been adopted in [30] to ensure asymptotic stability of a one-dimensional one-phase nonlinear Stefan problem assuming a prior known moving boundary and deriving the manipulated input from the solutions of the inverse problem. However, the series representation introduced in [30] leads to highly complex solutions that reduce controller design possibilities.

For control objectives, infinite-dimensional frameworks that lead to significant challenges in the process characterization have been developed for the stabilization of the temperature profile and the moving interface of the Stefan problem. An enthalpy-based boundary feedback control law that ensures asymptotical stability of the temperature profile and the moving boundary at the desired reference, has been employed in [31]. Lyapunov analysis is performed in [26] based on a geometric control approach which enables to adjust the position of a liquid-solid interface to the desired setpoint while exponentially stabilizing the L_2-norm of the distributed temperature. However, the results in [26] are stated based on physical assumptions on the liquid temperature being greater than the melting point, which needs to be guaranteed by proving strictly positive boundary input.

Backstepping controller design employs an invertible transformation that maps an original system into a stable target system. During the past few decades, such a controller design technique has been intensely exploited for the boundary control of diffusion PDEs defined on a fixed spatial domain as firstly introduced in [5] for the control of a heat equation via measurement of domain-average temperature. For a class

S. Koga and M. Krstic are with the Department of Mechanical and Aerospace Engineering, University of California at San Diego, La Jolla, CA, 92093-0411 USA (e-mail: skoga@ucsd.edu; krstic@ucsd.edu).

M. Diagne is with the Department of Mechanical Aerospace and Nuclear Engineering of Rensselaer Polytechnic Institute , Troy, NY 12180-3590, USA (email: diagnm@rpi.edu).

of one-dimensional linear parabolic partial integro-differential equations, a state-estimator called backstepping observer was introduced in [34], which can be combined to the earlier state feedback boundary controller designed for an identical system [33] to systematically construct output feedback regulators. Over the same period, reaction-advection-diffusion systems with space-dependent thermal conductivity or time-dependent reactivity coefficient were studied in [35], and parabolic PDEs containing unknown destabilizing parameters affecting the interior of the domain or unknown boundary parameters were adaptively controlled in [22], [36], [37] combining the backstepping control with passive or swapping identifiers.

Results devoted to the backstepping stabilization of coupled systems described by a diffusion PDE in cascade with a linear ODE has been primarily presented in [18] with Dirichlet type of boundary interconnection and extended to Neumann boundary interconnection in [40], [41]. For systems relevant with Stefan problem, [15] designed a backstepping output feedback controller that ensures the exponential stability of an unstable parabolic PDE on *a priori* known dynamics of moving interface which is assumed to be an analytic function in time. Moreover, for PDE-ODE cascaded systems under a state-dependent moving boundary, [6] derived a local stability result for nonlinear ODEs with actuator dynamics governed by a wave PDE defined on a time- and state-dependent moving domain. Such a technique is based on the input delay and wave compensation for nonlinear ODEs designed in [3], [19] and its extension to state-dependent input delay compensation for nonlinear ODEs provided by [2]. While the results in [6] and [2] that cover state-dependence problems do not ensure global stabilization due to a so-called feasibility condition that needs to be satisfied *a priori*, such a restriction was recently unlocked in [11] which provides a global stability result. However, the result in [11] is limited to the case of hyperbolic PDE in cascade with a nonlinear ODE.

b) Results and contributions: Our previous result in [16] is the first contribution in which global exponential stability of the Stefan problem with an implicitly given moving interface motion is established without imposing any *a priori* given restriction under a state feedback design of a Neumann boundary control, and in [17] we developed the design of an observer-based output feedback control. This paper extends the results in [16] and [17] by:

- providing the robustness analysis of the closed-loop system to the plant parameters' mismatch under the state feedback control,
- introducing a Dirichlet boundary actuation to design the state feedback, observer-based output feedback, and the robustness analysis under the state feedback control,
- and considering a Robin boundary actuation for the design of state feedback control motivated by metal additive manufacturing.

First, a state feedback control law that requires the measurement of the liquid phase temperature profile and the moving interface position is constructed using a novel nonlinear backstepping transformation. The proposed state feedback controller achieves exponential stabilization of the temperature profile and the moving interface to the desired setpoint in $\mathcal{H}_1$-norm under the least restrictive condition on the setpoint imposed by energy conservation law. Robustness of the state feedback controller to thermal diffusivity and latent heat of fusion mismatch is also characterized by explicitly given bounds of the uncertainties' magnitude. Second, an exponential stable state observer which reconstructs the entire distributed temperature profile based solely on the measurements of the interface position and the temperature gradient at the interface is constructed using the novel backstepping transformation. Finally, combining the state feedback law with the state estimator, the exponential stabilization of the estimation error, the temperature profile, and the moving interface to the setpoint in the $\mathcal{H}_1$-norm is proved under some explicitly given restrictions on the observer gain and the setpoint.

For the unperturbed Stefan problem, well-posedness of the classical solution of the closed-loop system is proved under the state feedback control via a Neumann boundary actuation. While well-posedness issues are important to some extents, due to the fact that the presented results are dedicated to the design of stabilizing controllers rather than the analysis, the well-posedness of the closed-loop system is assumed to hold for the output feedback and the robustness study.

c) Organizations: The one-phase Stefan problem with a Neumann boundary actuation is presented in Section II, and its open-loop stability is discussed in Section III. The full-state feedback controller is constructed in Section IV with a robustness analysis to parameters' perturbations. Section V explains the observer design and Section VI presents the observer-based output feedback control. In Section VII, both state feedback and output feedback are derived by considering a Dirichlet boundary actuation and robustness analysis is provided for the state feedback case. Section VIII presents the state feedback control law for a Robin boundary actuation. Simulations to support the theoretical results are given in Section IX. The paper ends with final remarks and future directions in Section X.

d) Notations: Throughout this paper, partial derivatives and several norms are denoted as

$$u_t(x,t) = \frac{\partial u}{\partial t}(x,t), \quad u_x(x,t) = \frac{\partial u}{\partial x}(x,t),$$

$$||u||_{L_2} = \sqrt{\int_0^{s(t)} u(x,t)^2 dx}, \quad ||u||_{\mathcal{H}_1} = \sqrt{||u||_{L_2}^2 + ||u_x||_{L_2}^2}$$

PART I: NEUMANN BOUNDARY ACTUATION

In this first part, we design a boundary controller for the Stefan problem with a Neumann boundary actuation.

II. DESCRIPTION OF THE PHYSICAL PROCESS

A. Phase change in a pure material

The one-dimensional Stefan problem is defined as the physical model which describes the melting or the solidification mechanism in a pure one-component material of length L in one dimension as depicted in Fig. 1. The dynamics of the process depends strongly on the evolution in time of the moving interface (here reduced to a point) at which phase transition

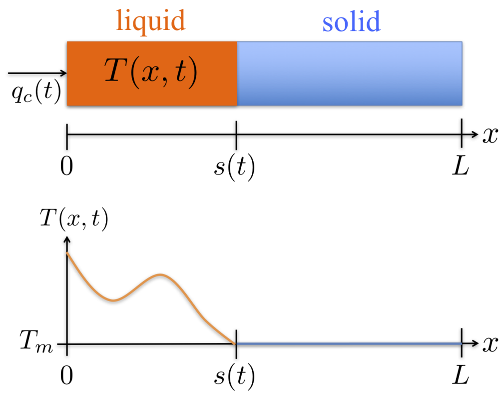

Fig. 1: Schematic of 1D Stefan problem.

from liquid to solid (or equivalently, in the reverse direction) occurs. Therefore, the melting or solidification mechanism which takes place in the physical domain $[0, L]$, induces the existence of two complementary time-varying sub-domains, namely, $[0, s(t)]$ occupied by the liquid phase, and $[s(t), L]$ by the solid phase. Assuming a temperature profile uniformly equivalent to the melting temperature in the solid phase, a dynamical model associated with the melting phenomenon (see Fig. 1) involves only the thermal behavior of the liquid phase. At a fundamental level, the thermal conduction for a melting component obeys the well known Fourier's law

$$q(x,t) = -kT_x(x,t), \tag{1}$$

where $q(x,t)$ is a heat flux profile, k is the thermal conductivity, and $T(x,t)$ is a temperature profile. Considering a melting material with a density ρ and heat capacity $C_{\rm p}$, in the open domain $(0, s(t))$, the local energy conservation law is given by

$$\rho C_{\rm p} T_t(x,t) = -q_x(x,t). \tag{2}$$

Assuming that the temperature in the liquid phase is not lower than the melting temperature of the material $T_{\rm m}$ and combining (1) and (2), one can derive the heat equation of the liquid phase as follows

$$T_t(x,t) = \alpha T_{xx}(x,t), \quad 0 \le x \le s(t), \quad \alpha := \frac{k}{\rho C_{\rm p}}, \tag{3}$$

with the boundary conditions

$$-kT_x(0,t) = q_{\rm c}(t), \tag{4}$$
$$T(s(t),t) = T_{\rm m}, \tag{5}$$

and the initial conditions

$$T(x,0) = T_0(x), \quad s(0) = s_0, \tag{6}$$

where $q_{\rm c}(t)$ is a controlled heat flux entering the system at the boundary $x = 0$. Moreover, the local energy balance at the position of the liquid-solid interface $x = s(t)$ leads to the Stefan condition defined as the following nonlinear ODE

$$\dot{s}(t) = -\beta T_x(s(t),t), \quad \beta := \frac{k}{\rho \Delta H^*}, \tag{7}$$

where ΔH^* denotes the latent heat of fusion. Equation (7) expresses the velocity of the liquid-solid moving interface.

For the sake of brevity, we refer the readers to [14], where the Stefan condition is derived for a solidification process.

The classical solution to the Stefan problem and the well-posedness (existence and uniqueness) were developed in [12] as stated in Appendix A.

B. Some key properties of the physical model

For a homogeneous melting material, the Stefan problem presented in Section II exhibits some important properties that are discussed in the following remarks.

Remark 1. As the moving interface $s(t)$ governed by (7) is unknown explicitly, the problem defined in (3)–(7) is a nonlinear problem.

Remark 2. Due to the so-called isothermal interface condition that prescribes the melting temperature $T_{\rm m}$ at the interface through (5), the governing equations (3)–(7) of the Stefan problem is a reasonable model only if the following condition holds:

$$T(x,t) \ge T_{\rm m}, \quad \text{for all} \quad x \in [0, s(t)]. \tag{8}$$

The model is valid if and only if the liquid temperature is greater than the melting temperature and such a condition yields the following property on moving interface.

Corollary 1. *If the model validity condition* (8) *holds, then the moving interface is monotonically nondecreasing, i.e.,*

$$\dot{s}(t) \ge 0, \quad \textit{for all} \quad t \ge 0. \tag{9}$$

Corollary 1 is established using Hopf's Lemma and a detailed proof can be found in [14]. Hence, it is plausible to impose the following assumption on the initial values.

Assumption 1. *The initial interface position satisfies* $s_0 > 0$ *and the Lipschitz continuity of* $T_0(x)$ *holds, i.e.,*

$$0 \le T_0(x) - T_{\rm m} \le H(s_0 - x). \tag{10}$$

Assumption 1 ensures the weak differentiability of $T_0(x)$ and hence $T_0(x) \in H^1_{[0,s_0]}$, which is physically reasonable and consistent with Remark 2. For the validity of the model (3)–(7), we recall the following lemma.

Lemma 1. *If there is a unique classical solution of* (3)–(7)*, then for any* $q_{\rm c}(t) > 0$ *on the finite time interval* $(0, \bar{t})$*, the condition* (8) *holds.*

The proof of Lemma 1 is based on Maximum principle as shown in [14]. In this paper, we focus on this melting problem which requires the positivity of the boundary heat flux.

III. Control Problem and an Open-Loop Stability

A. Problem statement

The steady-state solution $(T_{\rm eq}(x), s_{\rm eq})$ of the system (3)–(7) with zero manipulating heat flux $q_{\rm c}(t) = 0$ yields a uniform melting temperature $T_{\rm eq}(x) = T_{\rm m}$ and a constant interface position given by the initial data. Hence, the system (3)–(7) is marginally stable. In this section, we consider the asymptotical stabilization of the interface position $s(t)$ at a desired reference setpoint $s_{\rm r}$, while the equilibrium temperature profile is maintained at $T_{\rm m}$. Thus, the control objective is formulated as

$$\lim_{t\to\infty} s(t) = s_{\rm r}, \tag{11}$$

$$\lim_{t\to\infty} T(x,t) = T_{\rm m}. \tag{12}$$

B. Setpoint restriction by energy conservation principle

The positivity of the manipulated heat flux in Lemma 1 imposes a restriction on the setpoint given that the system (3)–(7) satisfies an energy conservation that is given by

$$\frac{d}{dt}\left(\frac{k}{\alpha}\int_0^{s(t)}(T(x,t)-T_{\rm m})dx + \frac{k}{\beta}s(t)\right) = q_{\rm c}(t). \tag{13}$$

The left-hand side of (13) denotes the growth of internal energy composed of the specific heat and the latent heat, and its right-hand side denotes the external work provided by the injected heat flux. Integrating (13) in t from 0 to ∞ and substituting (11) and (12), one can deduce that the heat flux $q_c(t)$ which drives the system (3)–(7) to the desired setpoint, satisfies the following relation

$$\frac{k}{\beta}(s_{\rm r}-s_0) - \frac{k}{\alpha}\int_0^{s_0}(T_0(x)-T_{\rm m})dx = \int_0^{\infty} q_{\rm c}(t)dt. \tag{14}$$

From relation (14), one can deduce that for any positive heat flux control $q_{\rm c}(t) > 0$, the internal energy for a given setpoint must be greater than the initial internal energy. Thus, the following assumption is required.

Assumption 2. *The setpoint $s_{\rm r}$ is chosen to satisfy*

$$s_{\rm r} > s_0 + \frac{\beta}{\alpha}\int_0^{s_0}(T_0(x)-T_{\rm m})dx. \tag{15}$$

Therefore, Assumption 2 stands as the least restrictive condition for the choice of setpoint and can be consequently viewed as a setpoint restriction.

C. Open-loop setpoint control law

For any given open-loop control law $q_{\rm c}(t)$ satisfying (14), the asymptotical stability of the system (3)–(7) at $s_{\rm r}$ can be established and the following lemma holds.

Lemma 2. *Consider an open-loop setpoint control law $q_{\rm c}^\star(t)$ which satisfies* (14)*. Then, the interface converges asymptotically to the prescribed setpoint $s_{\rm r}$ and consequently, conditions* (11) *and* (12) *hold.*

The proof of Lemma 2 can be derived straightforwardly from (14). To illustrate the introduced concept of open-loop "energy shaping control" action, we define ΔE as the left-hand side of (14), i.e.,

$$\Delta E = \frac{k}{\beta}(s_{\rm r}-s_0) - \frac{k}{\alpha}\int_0^{s_0}(T_0(x)-T_{\rm m})dx. \tag{16}$$

For instance, the rectangular pulse control law given by

$$q_{\rm c}^\star(t) = \left\{\begin{array}{lll} \bar{q} & \text{for} & t\in[0,\Delta E/\bar{q}] \\ 0 & \text{for} & t > \Delta E/\bar{q} \end{array}\right\} \tag{17}$$

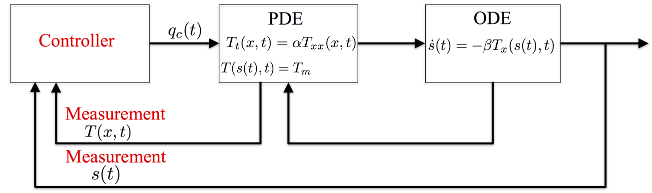

Fig. 2: Block diagram of the state feedback closed-loop control.

satisfies (16) for any choice of the boundary heat flux $\bar{q}$ and thereby, ensures the asymptotical stability of (3)–(7) to the setpoint $(T_{\rm m}, s_{\rm r})$.

IV. State Feedback Control

It is remarkable that adopting an open-loop control strategy such as the rectangular pulse (17), does not allow to improve the convergence speed. Moreover, the physical parameters of the model need to be known accurately. In engineering process, the practical implementation of an open-loop control is limited by performance and robustness issues, thus closed-loop control laws have to be designed to deal with such limitations.

In this section, we focus on the design of closed-loop backstepping control law for the one-phase Stefan problem in order to achieve faster exponential convergence to the desired setpoint $(T_{\rm m}, s_{\rm r})$ while ensuring the robustness of the closed-loop system to the uncertainty of the physical parameters. We recall that from a physical point of view, for any positive heat flux $q_{\rm c}(t)$, the irreversibility of the process restrict *a priori* the choice of the desired setpoint $s_{\rm r}$ to satisfy (15).

Assuming that the liquid temperature profile $T(x,t)$ and the position of the moving interface $s(t)$ are measured $\forall x \in [0, s(t)]$ and $\forall t \geq 0$, the following theorem holds:

Theorem 1. *Consider a closed-loop system consisting of the plant* (3)–(7) *and the control law*

$$q_{\rm c}(t) = -c\left(\frac{k}{\alpha}\int_0^{s(t)}(T(x,t)-T_{\rm m})dx + \frac{k}{\beta}(s(t)-s_{\rm r})\right), \tag{18}$$

where $c > 0$ is an arbitrary controller gain. Let Assumption 1 and Assumption 2 hold, and assume that the initial conditions $(T_0(x), s_0)$ are compatible with the control law. Then, the closed-loop system has a unique classical solution, which satisfies the model validity condition (8)*, and is exponentially stable in the sense of the norm*

$$||T-T_{\rm m}||^2_{\mathcal{H}_1} + (s(t)-s_{\rm r})^2. \tag{19}$$

The proof of Theorem 1 is established by following steps:

- A backstepping transformation for moving boundary PDEs and the associated inverse transformation are constructed for a reference error system (see Section IV-A).
- Physical constraints that guarantee the positivity of the boundary heat flux under closed-loop control are derived (see Section IV-B).

- The stability analysis of the target system that induces the stability of the original reference error system is performed (see Section IV-C).

A. Backstepping transformation for moving boundary PDEs

1) Reference error system: For a given reference setpoint $(T_{\rm m}, s_{\rm r})$, we define the reference errors as

$$u(x,t) = T(x,t) - T_{\rm m}, \quad X(t) = s(t) - s_{\rm r}, \tag{20}$$

respectively. Then, the reference error system associated with the coupled system (3)–(7) is written as

$$u_t(x,t) = \alpha u_{xx}(x,t), \quad 0 \le x \le s(t), \tag{21}$$
$$-k u_x(0,t) = q_{\rm c}(t), \tag{22}$$
$$u(s(t),t) = 0, \tag{23}$$
$$\dot{X}(t) = -\beta u_x(s(t),t). \tag{24}$$

2) Direct transformation: Next, we introduce the following backstepping transformation [1]

$$w(x,t) = u(x,t) - \frac{\beta}{\alpha}\int_x^{s(t)} \phi(x-y)u(y,t)dy - \phi(x - s(t))X(t), \tag{25}$$
$$\phi(x) = \frac{c}{\beta}x, \tag{26}$$

which transforms system (21)–(24) into the following

$$w_t(x,t) = \alpha w_{xx}(x,t) + \frac{c}{\beta}\dot{s}(t)X(t), \tag{27}$$
$$w_x(0,t) = 0, \tag{28}$$
$$w(s(t),t) = 0, \tag{29}$$
$$\dot{X}(t) = -cX(t) - \beta w_x(s(t),t). \tag{30}$$

The derivation of the explicit gain kernel function (26) is given in Appendix B-1.

3) Inverse transformation: The inverse transformation of (25) is given by

$$u(x,t) = w(x,t) + \frac{\beta}{\alpha}\int_x^{s(t)} \psi(x-y)w(y,t)dy + \psi(x - s(t))X(t), \tag{31}$$
$$\psi(x) = \frac{c}{\beta}\sqrt{\frac{\alpha}{c}}\sin\left(\sqrt{\frac{c}{\alpha}}x\right). \tag{32}$$

As for the direct transformation, the derivation of the inverse transformation (31) is detailed in Appendix B-2.

Remark 3. Replacing $s(t)$ with $X(t) + s_{\rm r}$ in the transformations (25) and (31), one can easily see that the transformations (25) and (31) are nonlinear.

The nonlinearity of the direct and inverse transformations implies that the stability properties of (u,X)-system and (w,X)-system are equivalent only if both transformations are bounded, which is shown in Appendix C-2.

[1]The transformation (25) is an extension of the one initially introduced in [18], and lately employed in [40], [41] considering the moving boundary.

B. Physical constraints

As stated in Remark 2 and Lemma 1, a strictly positive heat flux $q_{\rm c}(t)$ is required not to violate the condition of the model validity (8). Based on the aforementioned condition and knowing that the moving interface dynamics is monotonically nondecreasing (9), the interface $s(t)$ cannot exceed the reference setpoint $s_{\rm r}$, namely, the stabilization has to be realized without overshoots. In this section, we establish that the state feedback control law (18) achieves the control objective (11) and (12), while satisfying the following "physical constraints"

$$q_{\rm c}(t) > 0, \quad \forall t > 0 \tag{33}$$
$$s_0 < s(t) < s_{\rm r}, \quad \forall t > 0 \tag{34}$$

Proposition 1. *Under Assumption 2, the closed-loop responses of the plant* (3)–(7) *with the control law* (18) *has a unique classical solution and satisfies the physical constraints* (33) *and* (34)*, and hence, conditions* (8) *and* (9) *hold.*

Proof: Taking the time derivative of (18) along the solution of (3)–(7), we have

$$\dot{q}_{\rm c}(t) = -c q_{\rm c}(t). \tag{35}$$

Solving (35) leads to

$$q_{\rm c}(t) = q_{\rm c}(0)e^{-ct}. \tag{36}$$

Since the setpoint restriction (15) implies $q_{\rm c}(0) > 0$, the closed-loop solution of (3)–(7) with the control law (18) is equivalent to the solution of (3)–(7) with the control law (36) that is strictly positive and continuously differentiable. Hence, using Lemma 8 in Appendix A, one can deduce that the closed-loop system has a unique classical solution. Then, using Lemma 1 and Corollary 1, conditions (8) and (9) are satisfied. Applying (33) and (8) to the control law (18), we obtain $s(t) < s_{\rm r}$, $\forall t > 0$. In addition, (9) implies that $s_0 < s(t)$. Combining these two later inequalities leads to (34). ■

Remark 4. The proposed control law (18) is applicable when the system is subject to input and state constraints by restricting the controller gain c appropriately. For instance, if the heat flux is subject to the saturation constraint $0 \le q_{\rm c}(t) \le q_{\max}$, by setting the gain of (18) as $0 < c \le \frac{q_{\max}}{\Delta E}$, where ΔE is defined by (16), a practically implementable controller is constructed. Also, by virtue of Maximum principle, the bounded input yields an estimate of the temperature profile as $T(x,t) - T_{\rm m} \le K(s(t) - x)$, $\forall x \in (0, s(t))$, $\forall t > 0$, where $K = \max\{H, c\Delta E/k\}$ and H is defined in (10). Hence, under the state constraint $T_{\rm m} \le T(x,t) \le T_{\rm b}$ where $T_{\rm b}$ is the upper bound of the temperature (physically, $T_{\rm b}$ can be viewed as a boiling temperature), by setting $0 < c \le k(T_{\rm b} - T_{\rm m})/\Delta E s_{\rm r}$, the closed-loop system satisfies the state constraint.

In the next section, the inequalities (9) and (34) are used to establish the Lyapunov stability of the target system (27)–(30).

C. Stability analysis

In the following, we establish the exponential stability of the closed-loop control system consisting of (3)–(7) together with

(18), with respect to the $\mathcal{H}_1$-norm of the temperature and the moving boundary based on the analysis of the target system (27)–(30). We consider a functional

$$V =\frac{1}{2}||w||^2_{\mathcal{H}_1} + \frac{p}{2}X(t)^2, \tag{37}$$

where $p = \frac{c\alpha}{4\beta^2 s_{\rm r}}$. Taking the time derivative of (37) along the solution of the target system (27)–(30) and applying Young's, Cauchy-Schwarz, Poincare's and Agmon's inequalities, with the help of (9) and (34), we have

$$\dot{V} \leq - bV + a\dot{s}(t)V, \tag{38}$$

where $a = \max\left\{s_{\rm r}^2, \frac{8s_{\rm r}c}{\alpha}\right\}$, $b = \min\left\{\frac{\alpha}{4s_{\rm r}^2}, c\right\}$. The detailed derivation of (38) is given in Appendix C-1.

However, the second term of the right-hand side of (38) does not enable to directly conclude the exponential stability. To deal with it, we introduce a new Lyapunov function W such that

$$W = Ve^{-as(t)}. \tag{39}$$

The time derivative of (39) is written as

$$\dot{W} = \left(\dot{V} - a\dot{s}(t)V\right) e^{-as(t)}, \tag{40}$$

and using (38) the following estimate can be deduced

$$\dot{W} \leq -bW. \tag{41}$$

Hence, $W(t) \leq W(0)e^{-bt}$, and using (34) and (39), we obtain

$$V(t) \leq e^{as_{\rm r}}V(0)e^{-bt}. \tag{42}$$

From the definition of V in (37) the following holds

$$||w||^2_{\mathcal{H}_1} + pX(t)^2 \leq e^{as_{\rm r}}\left(||w_0||^2_{\mathcal{H}_1} + pX(0)^2\right) e^{-bt}. \tag{43}$$

Finally, with the help of (34), the direct transformation (25)–(26) and its associated inverse transformation (31)–(32) combined with Young's and Cauchy-Schwarz inequalities, enable to state the existence of a positive constant $D > 0$ such that

$$||u||^2_{\mathcal{H}_1} + X(t)^2 \leq D\left(||u_0||^2_{\mathcal{H}_1} + X(0)^2\right) e^{-bt}, \tag{44}$$

which completes the proof of Theorem 1. The detailed derivation of (44) from (43) is provided in Appendix C-2.

Hereafter, we assume the compatibility condition between the initial data of the plant and the controller and the well-posedness of the classical solution of the closed-loop system.

Next, we show the robustness of the closed-loop system.

D. Robustness to parameters' uncertainty

In this section, we prove the robustness of the controller (18) when the plant's parameters α and β are likely not deterministically known. In other words, we account for perturbations caused by uncertainties of the thermal diffusivity and the latent heat of fusion. Hence, we consider the following closed-loop system

$$T_t(x,t) =\alpha(1+\varepsilon_1)T_{xx}(x,t), \quad 0 \leq x \leq s(t), \tag{45}$$
$$-kT_x(0,t) =q_{\rm c}(t), \tag{46}$$
$$T(s(t),t) =T_{\rm m}, \tag{47}$$
$$\dot{s}(t) =- \beta(1+\varepsilon_2)T_x(s(t),t), \tag{48}$$

with the control law (18), where ε_1 and ε_2 are parameters' perturbation such that $\varepsilon_1 > -1$ and $\varepsilon_2 > -1$.

Theorem 2. *Consider a closed-loop system* (45)–(48) *and the control law* (18) *under Assumption 1 and 2. Then, for any pair of perturbation* $(\varepsilon_1, \varepsilon_2)$ *such that* $\varepsilon_1 \geq \varepsilon_2$ *and for any control gain* c *satisfying* $0 < c \leq c^*$ *where*

$$c^* = \left(\frac{3}{10}\right)^{1/4} \frac{\alpha}{8s_{\rm r}^2}\frac{1+\varepsilon_1}{\varepsilon_1-\varepsilon_2}, \tag{49}$$

the closed-loop system is exponentially stable in the sense of the $\mathcal{H}_1$ *norm* (19).

Proof: Using the backstepping transformation (25), the target system associated to (45)–(48) is defined as follows

$$\begin{aligned} w_t(x,t) =&\alpha(1+\varepsilon_1)w_{xx}(x,t) + \frac{c}{\beta}\dot{s}(t)X(t) \\ &+ \frac{c}{\beta}\frac{\varepsilon_1-\varepsilon_2}{1+\varepsilon_2}\dot{s}(t)(x-s(t)), \end{aligned} \tag{50}$$
$$w(s(t),t) =0, \quad w_x(0,t) = 0, \tag{51}$$
$$\dot{X}(t) =- c(1+\varepsilon_2)X(t) - \beta(1+\varepsilon_2)w_x(s(t),t). \tag{52}$$

Next, we prove that the control law (18) applied to the perturbed system (45)–(48), satisfies (33) and (34). Taking the time derivative of (18) along with (45)–(48), we arrive at

$$\dot{q}_{\rm c}(t) = -c(1+\varepsilon_1)q_{\rm c}(t) - ck\left(\varepsilon_1-\varepsilon_2\right)u_x(s(t),t). \tag{53}$$

The positivity of the control law (18) applied to the perturbed system (45)–(48) can be shown using a contradiction argument. Assume that there exists $t_1 > 0$ such that $q_{\rm c}(t) > 0$, $\forall t \in (0,t_1)$ and $q_{\rm c}(t_1) = 0$. Then, Lemma 1 and Hopf's Lemma leads to $u_x(s(t),t) < 0$, $\forall t \in (0,t_1)$. Since $\varepsilon_1 \geq \varepsilon_2$, (53) implies that

$$\dot{q}_{\rm c}(t) \geq -c(1+\varepsilon_1)q_{\rm c}(t), \quad \forall t \in (0,t_1). \tag{54}$$

Using comparison principle, (54) and Assumption 2 leads to $q_{\rm c}(t_1) \geq q_{\rm c}(0)e^{-c(1+\varepsilon_1)t_1} > 0$. Thus $q_{\rm c}(t_1) \neq 0$ which is in contradiction with the assumption $q_{\rm c}(t_1) = 0$. Consequently, (33) holds by this contradiction argument. Accordingly, (34) is established using (33) and the control law (18).

Now, consider a functional

$$V_\varepsilon = \frac{d}{2}||w||^2_{L_2} + \frac{1}{2}||w_x||^2_{L_2} + \frac{p}{2}X(t)^2, \tag{55}$$

where the parameters d and p are chosen as $p = \frac{c\alpha(1+\varepsilon_1)}{8s_{\rm r}(1+\varepsilon_2)\beta^2}$, $d = \frac{160s_{\rm r}^2c^2(\varepsilon_1-\varepsilon_2)^2}{\alpha^2(1+\varepsilon_1)^2}$. Taking the time derivative of (55) along the solution of (50)–(52) and applying the Young's, Cauchy-Schwarz, Poincare's and Agmon's inequalities, we get

$$\begin{aligned} \dot{V}_\varepsilon \leq &- d\left(\frac{\alpha(1+\varepsilon_1)}{4}\right)||w_x||^2_{L_2} \\ &- \frac{\alpha(1+\varepsilon_1)}{12}\left(4 - \left(\frac{c}{c^*}\right)^4\right)||w_{xx}||^2_{L_2} \end{aligned}$$

$$- \frac{c^2}{\beta^2}\frac{\alpha(1+\varepsilon_1)}{64 s_{\rm r}}\left(2-\left(\frac{c}{c^*}\right)^4\right)X(t)^2 + \dot{s}(t)\left\{d^2 s_{\rm r}^2||w||_{L_2}^2 + \frac{c^2}{\beta^2}X(t)^2\right\}. \quad (56)$$

From (56) we deduce that for all $0 < c < c^*$, there exists positive parameters $a > 0$ and $b > 0$ such that

$$\dot{V}_\varepsilon \leq -bV_\varepsilon + a\dot{s}(t)V_\varepsilon. \quad (57)$$

The exponential stability of the target system (50)–(52) can be straightforwardly established following the proof procedure used in (39)–(43), which completes the proof of Theorem 2. ■

V. State Estimation Design

A. Problem statement and main result

The computation of the controller (18) requires the measurement of both the distributed temperature profile $T(x,t)$ along the domain $(0, s(t))$ and the moving interface position $s(t)$, which relatively limits its practical relevance. With the aim of designing an output feedback control law that requires fewer measurements, we derive an estimator of the temperature profile based only on the measurements of moving interface position $s(t)$ and the temperature gradient at the interface $T_x(s(t),t)$. Denoting the estimates of the temperature $\hat{T}(x,t)$, the following theorem holds:

Theorem 3. *Consider the plant* (3)–(7) *with the measurements* $Y_1(t) = s(t)$, $Y_2(t) = T_x(s(t),t)$, *and the following observer*

$$\hat{T}_t(x,t) = \alpha\hat{T}_{xx}(x,t) + p_1(x, Y_1(t))\left(Y_2(t) - \hat{T}_x(Y_1(t),t)\right), \quad (58)$$

$$-k\hat{T}_x(0,t) = q_{\rm c}(t), \quad (59)$$

$$\hat{T}(Y_1(t),t) = T_{\rm m}, \quad (60)$$

where $x \in [0, Y_1(t)]$, *and the observer gain* $p_1(x, Y_1(t))$ *is*

$$p_1(x, Y_1(t)) = -\lambda Y_1(t)\frac{I_1\left(\sqrt{\frac{\lambda}{\alpha}\left(Y_1(t)^2 - x^2\right)}\right)}{\sqrt{\frac{\lambda}{\alpha}\left(Y_1(t)^2 - x^2\right)}}, \quad (61)$$

with a gain parameter $\lambda > 0$. *Assume that the two physical constraints* (33) *and* (34) *are satisfied. Then, for all* $\lambda > 0$, *the observer error system has a unique classical solution and is exponentially stable in the sense of the norm*

$$||T - \hat{T}||_{\mathcal{H}_1}^2. \quad (62)$$

Since the observer PDE (58)–(60) is a cascaded system of the plant PDE-ODE (3)–(7), the observer state $\hat{T}(x,t)$ admits a classical solution only if the plant states $(T(x,t), s(t))$ admits a classical solution.

The proof of Theorem 3 is established later in Section V.

B. Observer design and backstepping transformation

1) Observer design and observer error system: For the reference error system, namely, the u-system (21)–(24), we consider the following observer:

$$\hat{u}_t(x,t) = \alpha\hat{u}_{xx}(x,t) + p_1(x, Y_1(t))\left(Y_2(t) - \hat{u}_x(Y_1(t),t)\right), \quad (63)$$

$$\hat{u}(Y_1(t),t) = 0, \quad (64)$$

$$-k\hat{u}_x(0,t) = q_{\rm c}(t), \quad (65)$$

where $p_1(x, Y_1(t))$ is the observer gain to be determined. Let $\tilde{u}(x,t)$ be the estimation error of the u-system defined as

$$\tilde{u}(x,t) = u(x,t) - \hat{u}(x,t). \quad (66)$$

Combining (21)–(24) with (63)–(65) where $Y_1(t) = s(t)$, the $\tilde{u}$-system is written as

$$\tilde{u}_t(x,t) = \alpha\tilde{u}_{xx}(x,t) - p_1(x, s(t))\tilde{u}_x(s(t),t), \quad (67)$$

$$\tilde{u}(s(t),t) = 0, \quad \tilde{u}_x(0,t) = 0. \quad (68)$$

2) Direct transformation: As for the full-state feedback case, the following backstepping transformation for moving boundary PDEs

$$\tilde{u}(x,t) = \tilde{w}(x,t) + \int_x^{s(t)} P(x,y)\tilde{w}(y,t)dy, \quad (69)$$

is constructed to convert the following exponentially stable target system

$$\tilde{w}_t(x,t) = \alpha\tilde{w}_{xx}(x,t) - \lambda\tilde{w}(x,t), \quad (70)$$

$$\tilde{w}(s(t),t) = 0, \quad \tilde{w}_x(0,t) = 0. \quad (71)$$

into the $\tilde{u}$-system (67), (68). Taking the derivative of (69) with respect to t and x along the solution of (70), (71), respectively, for any continuous function $\tilde{w}(x,t)$, the gain kernel $P(x,y)$ and the observer gain λ must satisfy the following PDE

$$P_{xx}(x,y) - P_{yy}(x,y) + \frac{\lambda}{\alpha}P(x,y) = 0, \quad (72)$$

$$P(x,x) = \frac{\lambda}{2\alpha}x, \quad P_x(0,y) = 0, \quad (73)$$

$$p_1(x, s(t)) = -\alpha P(x, s(t)), \quad (74)$$

in order to map (67)–(68) into (70), (71). The solution to (72)–(73) is written as

$$P(x,y) = \frac{\lambda}{\alpha}y\frac{I_1\left(\sqrt{\frac{\lambda}{\alpha}(y^2 - x^2)}\right)}{\sqrt{\frac{\lambda}{\alpha}(y^2 - x^2)}}, \quad (75)$$

where $I_1(x)$ is a modified Bessel function of the first kind. Finally, using (74), the observer gain (61) is derived.

3) Inverse transformation : The inverse transformation that maps the $\tilde{w}$-system (70), (71) into the $\tilde{u}$-system (67), (68) is written as

$$\tilde{w}(x,t) = \tilde{u}(x,t) - \int_x^{s(t)} Q(x,y)\tilde{u}(y,t)dy, \quad (76)$$

where the gain kernel $Q(x,y)$ satisfies

$$Q_{xx}(x,y) - Q_{yy}(x,y) - \frac{\lambda}{\alpha}Q(x,y) = 0, \quad (77)$$

$$Q(x,x) = \frac{\lambda}{2\alpha}x, \quad Q_x(0,y) = 0. \tag{78}$$

The solution to (77), (78) is written as

$$Q(x,y) =\frac{\lambda}{\alpha}y\frac{J_1\left(\sqrt{\frac{\lambda}{\alpha}(y^2-x^2)}\right)}{\sqrt{\frac{\lambda}{\alpha}(y^2-x^2)}}, \tag{79}$$

where $J_1(x)$ is a Bessel function of the first kind.

C. Stability analysis

To show the stability of the target $\tilde{w}$-system (70), (71), we consider a functional

$$\tilde{V} =\frac{1}{2}||\tilde{w}||^2_{\mathcal{H}_1}. \tag{80}$$

Taking the time derivative of (80) along the solution of (70), (71) leads to

$$\dot{\tilde{V}} = -\alpha||\tilde{w}_x||^2_{\mathcal{H}_1} - \lambda||\tilde{w}||^2_{\mathcal{H}_1} - \frac{\dot{s}(t)}{2}\tilde{w}_x(s(t),t)^2. \tag{81}$$

Using (33) and applying Poincare's inequality, the following differential inequality in $\tilde{V}$ is derived

$$\dot{\tilde{V}} \leq -\left(\frac{\alpha}{4s_{\rm r}^2}+\lambda\right)\tilde{V}. \tag{82}$$

Hence, the origin of the target $\tilde{w}$-system (70), (71) is exponentially stable. Since the the inverse of the transformation (69) is given by (76), the exponential stability of the target $\tilde{w}$-system at the origin induces the exponential stability of the original $\tilde{u}$-system (67), (68) at the origin, with the help of (34), which completes the proof of Theorem 3.

VI. Observer-Based output feedback Control

An output feedback control law is constructed using the reconstruction of the estimated temperature profile through the exponentially convergent observer (58)–(60) with the measurements as shown in Fig. 3 and the following theorem holds:

Theorem 4. *Consider the closed-loop system* (3)–(7) *with the measurements* $Y_1(t) = s(t)$, $Y_2(t) = T_x(s(t),t)$, *and the observer* (58)–(60) *under the output feedback control law*

$$q_{\rm c}(t) = -c\left(\frac{k}{\alpha}\int_0^{s(t)}\left(\hat{T}(x,t)-T_{\rm m}\right)dx + \frac{k}{\beta}\left(s(t)-s_{\rm r}\right)\right). \tag{83}$$

Under Assumption 1 and assuming that the Lipschitz constant H *in* (10) *is known, for any initial temperature estimation* $\hat{T}_0(x)$*, any gain parameter of the observer* λ*, and any setpoint* $s_{\rm r}$ *satisfying*

$$T_{\rm m} + \hat{H}_l(s_0-x) \leq \hat{T}_0(x) \leq T_{\rm m} + \hat{H}_u(s_0-x), \tag{84}$$

$$\lambda <\frac{4\alpha}{s_0^2}\frac{\hat{H}_l - H}{\hat{H}_u}, \tag{85}$$

$$s_{\rm r} >s_0 + \frac{\beta s_0^2}{2\alpha}\hat{H}_u, \tag{86}$$

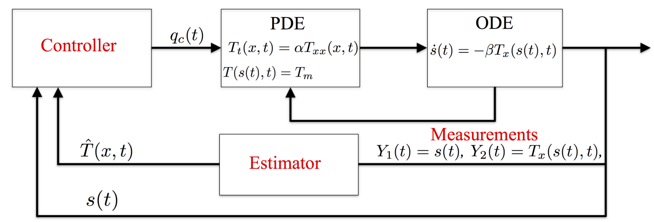

Fig. 3: Block diagram of observer design and output feedback.

respectively, where the parameters $\hat{H}_u$ *and* $\hat{H}_l$ *satisfy* $\hat{H}_u \geq \hat{H}_l > H$*, the closed-loop system is exponentially stable in the sense of the norm*

$$||T-\hat{T}||^2_{\mathcal{H}_1} + ||T-T_{\rm m}||^2_{\mathcal{H}_1} + (s(t)-s_{\rm r})^2. \tag{87}$$

The proof of Theorem 4 is derived by

- introducing a backstepping transformation and the associated target system,
- verifying the constraints (33) and (34),
- and establishing the Lyapunov stability proof.

A. Backstepping transformation

By equivalence, the transformation of the variables $(\hat{u}, X)$ into $(\hat{w}, X)$ is performed using the gain kernel functions of backstepping transformation (25). Thus,

$$\begin{aligned}\hat{w}(x,t) =&\hat{u}(x,t) - \frac{c}{\alpha}\int_x^{s(t)}(x-y)\hat{u}(y,t)dy\\ &- \frac{c}{\beta}(x-s(t))X(t). \end{aligned}\tag{88}$$

Taking the derivatives of (88) with respect to x and t along with the solution of (63)–(65) with the help of the transformation (69), the associated target system is obtained by

$$\begin{aligned}\hat{w}_t(x,t) =&\alpha\hat{w}_{xx}(x,t) + \frac{c}{\beta}\dot{s}(t)X(t)\\ &+ f(x,s(t))\tilde{w}_x(s(t),t), \end{aligned}\tag{89}$$

$$\hat{w}(s(t),t) =0, \quad \hat{w}_x(0,t) = 0, \tag{90}$$

$$\dot{X}(t) =-cX(t) - \beta\hat{w}_x(s(t),t) - \beta\tilde{w}_x(s(t),t), \tag{91}$$

where $f(x,s(t)) = P(x,s(t)) - \frac{c}{\alpha}\int_x^{s(t)}(x-y)P(y,s(t))dy - c(s(t)-x)$. Evaluating the spatial derivative of (88) at $x=0$, we derive the output feedback controller as

$$q_{\rm c}(t) = -ck\left(\frac{1}{\alpha}\int_0^{s(t)}\hat{u}(x,t)dx + \frac{1}{\beta}X(t)\right). \tag{92}$$

Following the procedure provided in Appendix B, the inverse transformation

$$\begin{aligned}\hat{u}(x,t) =&\hat{w}(x,t) + \frac{\beta}{\alpha}\int_x^{s(t)}\psi(x-y)\hat{w}(y,t)dy\\ &+ \psi(x-s(t))X(t), \end{aligned}\tag{93}$$

where the gain kernel (32) can be derived.

B. Physical constraints

In this section, we derive sufficient conditions to guarantee that the physical constraints (33) and (34) are not violated when the output feedback control law (92) is applied to the plant. First, we state the following lemma.

Lemma 3. *Suppose that* $\tilde{w}(0,t) < 0$*. Then, the solution to* (70)*,* (71) *satisfies* $\tilde{w}(x,t) < 0$*,* $\forall x \in (0, s(t))$*,* $\forall t > 0$*.*

The proof of Lemma 3 is constructed using the maximum principle [29]. Next, we state the following lemma.

Lemma 4. *For any initial temperature estimate* $\hat{T}_0(x)$ *and any observer gain parameter* λ *satisfying* (84) *and* (85)*, respectively, the following properties hold:*

$$\tilde{u}(x,t) < 0,\ \tilde{u}_x(s(t),t) > 0,\ \forall x \in (0, s(t)), \quad \forall t > 0. \tag{94}$$

Proof: Lemma 3 states that if $\tilde{w}(x,0) < 0$, then $\tilde{w}(x,t) < 0$. In addition, from (69), $\tilde{w}(x,t) < 0$ leads to $\tilde{u}(x,t) < 0$ due to the positivity of the solution to the gain kernel (75). Therefore, with the help of (76), we deduce that $\tilde{u}(x,t) < 0$ if the following holds

$$\tilde{u}(x,0) < \int_x^{s_0} Q(x,y)\tilde{u}(y,0)dy, \quad \forall x \in (0, s_0). \tag{95}$$

Considering the bound of the solution (79) under the condition (84), the sufficient condition for (95) to hold is given by (85), which restricts the gain λ. Thus, we have shown that conditions (84) and (85) lead to $\tilde{u}(x,t) < 0$, $\forall x \in (0, s(t))$, $\forall t > 0$. In addition, from the boundary condition (68) and Hopf's lemma, it follows that $\tilde{u}_x(s(t),t) > 0$. ■

The final step is to prove that the output feedback closed-loop system satisfies the physical constraints (33).

Proposition 2. *Suppose the initial values* $\hat{T}_0(x)$ *and* s_0 *satisfy* (84) *and the setpoint* $s_{\rm r}$ *is chosen to satisfy* (86)*. Then, the physical constraints* (33) *and* (34) *are satisfied by the closed-loop system consisting of the plant* (3)–(7)*, the observer* (58)–(60) *and the output feedback control law* (83)*.*

Proof: Taking the time derivative of (92) along with the solution (63)–(65), with the help of the observer gain (74), we derive the following differential equation:

$$\dot{q}_{\rm c}(t) = -cq_{\rm c}(t) + \left(1 + \int_0^{s(t)} P(x,s(t))dx\right)\tilde{u}_x(s(t),t). \tag{96}$$

From the positivity of the solution (75) and the Neumann boundary value (94), the following differential inequality holds

$$\dot{q}_{\rm c}(t) \geq -cq_{\rm c}(t). \tag{97}$$

Hence, if the initial values satisfy $q_{\rm c}(0) > 0$, equivalently (86) is satisfied from (92) and (84), we get

$$q_{\rm c}(t) > 0, \quad \forall t > 0. \tag{98}$$

Then, using (94) given in Lemma 4 and the positivity of $u(x,t)$ (see Lemma 1), the following inequality is established:

$$\hat{u}(x,t) > 0, \quad \forall x \in (0, s(t)), \quad \forall t > 0. \tag{99}$$

Finally, substituting the inequalities (98) and (99) into (92), we arrive at $X(t) < 0$, $\forall t > 0$, which guarantees that the second physical constraint (34) is satisfied. ■

C. Stability analysis

We consider a functional

$$\hat{V} = \frac{1}{2}||\hat{w}||^2_{\mathcal{H}_1} + \frac{p}{2}X(t)^2 + d\tilde{V}, \tag{100}$$

where $\tilde{V}$ is defined in (80), $d > 0$ is chosen to be large enough, and $p > 0$ is appropriately selected. Taking the time derivative of (80) along the solution of (89)–(91), and applying Young's, Cauchy-Schwarz, Poincare's, and Agmon's inequalities, with the help of (33) and (34), the following holds:

$$\dot{\hat{V}} \leq -b\hat{V} + a\dot{s}(t)\hat{V}, \tag{101}$$

where, $a = \max\left\{s_{\rm r}^2, \frac{16cs_{\rm r}}{\alpha}\right\}$, $b = \min\left\{\frac{\alpha}{8s_{\rm r}^2}, c, 2\lambda\right\}$. Hence, the origin of the $(\hat{w}, X, \tilde{w})$-system is exponentially stable. Since the inverse of the direct transformations (69) and (88) are given by (76) and (93), respectively, the exponential stability of $(\hat{w}, X, \tilde{w})$-system guarantees the exponential stability of $(\hat{u}, X, \tilde{u})$-system, which completes the proof of Theorem 4.

PART II: DIRICHLET AND ROBIN BOUNDARY ACTUATION

In PART I, a Neumann boundary actuation has been considered to design state and output feedback controllers. In this part, we focus on Dirichlet and Robin boundary actuations.

VII. DIRICHLET BOUNDARY ACTUATION

Some actuators such as a thermo-electric cooler require the direct controlling of the temperature at the boundary, which corresponds to a Dirichlet boundary control problem [4]. In this section, backstepping feedback control laws for the one-phase Stefan problem are constructed upon the boundary temperature actuation. We define the control problem consisting of the following system with the initial conditions (6):

$$T_t(x,t) = \alpha T_{xx}(x,t), \quad 0 \leq x \leq s(t), \tag{102}$$

$$T(0,t) = T_{\rm c}(t) + T_{\rm m}, \tag{103}$$

$$T(s(t),t) = T_{\rm m}, \tag{104}$$

$$\dot{s}(t) = -\beta T_x(s(t),t), \tag{105}$$

where $T_{\rm c}(t)$ is a controlled temperature relative to the melting temperature. Analogously to Lemma 1, the following lemma is stated.

Lemma 5. *If there is a unique classical solution to* (102)–(105)*, then for any* $T_{\rm c}(t) > 0$ *on the finite time interval* $(0, \bar{t})$*, the condition* (8) *holds.*

Similarly to Lemma 1, the proof of Lemma 5 is based on Maximum principle [29]. Therefore, the following condition is required to hold as a physical constraint

$$T_{\rm c}(t) > 0, \quad \forall t > 0. \tag{106}$$

A. Setpoint restriction

For boundary temperature control, the conservation law obeys the following equation

$$\frac{d}{dt}\left(\frac{1}{\alpha}\int_0^{s(t)} x(T(x,t)-T_{\rm m})dx + \frac{1}{2\beta}s(t)^2\right) = T_{\rm c}(t). \tag{107}$$

Considering the same control objective as in Section III, taking the limit of (107) from 0 to ∞ yields

$$\Delta E = \int_0^{\infty} T_{\rm c}(t)dt, \tag{108}$$

where $\Delta E := \frac{1}{2\beta}(s_{\rm r}^2 - s_0^2) - \frac{1}{\alpha}\int_0^{s_0} x(T_0(x)-T_{\rm m})dx$. Hence, by imposing the physical constraint (106), the least restrictive condition for the choice of setpoint is derived, and the open-loop stabilization is presented in the following.

Lemma 6. *Consider an open-loop setpoint control law $T_{\rm c}^{\star}(t)$ which satisfies* (108). *Then, for any setpoint $s_{\rm r}$ satisfying*

$$s_{\rm r} > \sqrt{s_0^2 + \frac{2\beta}{\alpha}\int_0^{s_0} x(T_0(x)-T_{\rm m})dx}, \tag{109}$$

the control objectives (11) *and* (12) *are satsified.*

As in Section III-C, a simple rectangular pulse input achieves (11) and (12). Such a control action given by

$$T_{\rm c}^{\star}(t) = \left\{ \begin{array}{lll} \bar{T} & \text{for} & t \in [0, \Delta E/\bar{T}] \\ 0 & \text{for} & t > \Delta E/\bar{T} \end{array} \right\}, \tag{110}$$

can be viewed as an open-loop "energy shaping" kind of approach.

B. State feedback controller design

Firstly, we suppose that the physical parameters are known and state the following theorem.

Theorem 5. *Consider a closed-loop system consisting of the plant* (102)–(105) *and the control law*

$$T_{\rm c}(t) = -c\left(\frac{1}{\alpha}\int_0^{s(t)} x\left(T(x,t)-T_{\rm m}\right)dx + \frac{1}{\beta}s(t)\left(s(t)-s_{\rm r}\right)\right), \tag{111}$$

where $c > 0$ is the controller gain under Assumption 1. Then, for any reference setpoint $s_{\rm r}$ and control gain c which satisfy

$$s_{\rm r} > s_0 + \frac{\beta}{\alpha}\int_0^{s_0} \frac{x}{s_0}(T_0(x)-T_{\rm m})dx, \tag{112}$$

$$c \le \frac{\alpha}{2\sqrt{2}s_{\rm r}}, \tag{113}$$

respectively, the closed-loop system is exponentially stable in the sense of the norm (19).

Proof: The backstepping transformation (25) leads to the following target system

$$w_t(x,t) = \alpha w_{xx}(x,t) + \frac{c}{\beta}\dot{s}(t)X(t), \tag{114}$$

$$w(s(t),t) = 0, \quad w(0,t) = 0, \tag{115}$$

$$\dot{X}(t) = -cX(t) - \beta w_x(s(t),t) \tag{116}$$

and the control law (111). Next, we show that the physical constraints (106) and (34) are insured if (112) holds. Taking the time derivative of (111), we have

$$\dot{T}_{\rm c}(t) = -cT_{\rm c}(t) - \frac{c}{\beta}\dot{s}(t)X(t). \tag{117}$$

Assume that $\exists t_2$ such that $T_{\rm c}(t) > 0$, $\forall t \in (0, t_2)$ and $T_{\rm c}(t_2) = 0$. Then, by Maximum principle, we get $u(x,t) > 0$ and $\dot{s}(t) > 0$ for $\forall t \in (0, t_2)$. Hence, $s(t) > s_0 > 0$. Applying these inequalities to (111), we deduce $X(t) < 0, \quad \forall t \in (0, t_2)$. Hence, (117) verifies the differential inequality $\dot{T}_{\rm c}(t) > -cT_{\rm c}(t), \quad \forall t \in (0, t_2)$. Comparison principle and (112) yield $T_{\rm c}(t_2) > T_{\rm c}(0)e^{-ct_2} > 0$ in contradiction to $T_{\rm c}(t_2) = 0$. Therefore, $\nexists t_2$ such that $T_{\rm c}(t) > 0$ for $\forall t \in (0, t_2)$ and $T_{\rm c}(t_2) = 0$, which implies $T_{\rm c}(t) > 0$, $\forall t > 0$ assuming (112). Finally, we consider a functional

$$V = \frac{d}{2}||w||_{L_2}^2 + \frac{1}{2}||w_x||_{L_2}^2 + \frac{p}{2}X(t)^2. \tag{118}$$

With an appropriate choice of the positive parameters d and p, the time derivative of (118) yields

$$\dot{V} \le -\left(\frac{\alpha}{2} - \sqrt{2}cs_{\rm r}\right)||w_{xx}||^2 - \frac{d\alpha}{2(4s_{\rm r}^2+1)}||w||_{\mathcal{H}_1}^2 - \frac{\alpha c^2}{4\beta^2}X(t)^2 + \dot{s}(t)\left(\frac{c^2}{\beta^2}X(t)^2 + \frac{d^2 s_{\rm r}^2}{2}||w||^2\right). \tag{119}$$

Thus, choosing the controller gain to satisfy (113), it can be verified that there exist positive constants b and a such that

$$\dot{V} \le -bV + a\dot{s}(t)V. \tag{120}$$

Similarly, in the Neumann boundary actuation case, under the physical constraint (106), the exponential stability of the target system (114)–(116) can be established, which completes the proof of Theorem 5. ■

C. Robustness to parameters' uncertainty

Next, we investigate the controller (111) to perturbations on the plant's physical parameters α and β, considering the following perturbed system

$$T_t(x,t) = \alpha(1+\varepsilon_1)T_{xx}(x,t), \quad 0 \le x \le s(t), \tag{121}$$

$$T(0,t) = T_{\rm c}(t) + T_{\rm m}, \tag{122}$$

$$T(s(t),t) = T_{\rm m}, \tag{123}$$

$$\dot{s}(t) = -\beta(1+\varepsilon_2)T_x(s(t),t) \tag{124}$$

where ε_1 and ε_2 are perturbation parameters such that $\varepsilon_1 > -1$ and $\varepsilon_2 > -1$.

Theorem 6. *Consider the closed-loop system consisting of the plant* (121)–(124) *and the control law* (111) *under the assumption on* (112) *to hold. Then, for any perturbations $(\varepsilon_1, \varepsilon_2)$ which satisfy $\varepsilon_1 \ge \varepsilon_2$, there exists $\bar{c}^* > 0$ such that for all controller gain c satisfying $0 < c \le \bar{c}^*$, the closed-loop system is exponentially stable in the sense of the norm* (19).

Proof: Note that the transformation (25)–(26) and the system described by (45), (47) and (48) are identical to the ones considered in Section IV-D. Moreover, only the boundary condition of the target system (50)–(52) at $x = 0$ is set to $w(0,t) = 0$, in order to match the temperature control problem.

Taking the time derivative of (111) along the system (45), (47)–(48), with the boundary condition (103), we obtain

$$\dot{T}_{\rm c}(t) = -c(1+\varepsilon_1)T_{\rm c}(t) - \frac{c}{\beta}\dot{s}(t)X(t) - c(\varepsilon_1-\varepsilon_2)u_x(s(t),t). \tag{125}$$

Thus, the inequality $\varepsilon_1 \geq \varepsilon_2$ enables to state the positivity of the controller $T_{\rm c}(t) > 0$ and the physical constraints (106) and (34) are verified.

Finally, we consider the functional defined in (55). With an appropriate choice of d and p and imposing $c < c_1$ where $c_1 := \frac{\alpha(1+\varepsilon_2)}{2\sqrt{2}s_{\rm r}}$, we have

$$\begin{aligned}\dot{V}_\varepsilon \leq &-\frac{d\alpha(1+\varepsilon_1)}{4}||w_x||_{L_2}^2 - \frac{\alpha(1+\varepsilon_1)}{8}\left(2-Ac^3\right)||w_{xx}||_{L_2}^2\\ &-\frac{c^2\alpha(1+\varepsilon_1)}{32\beta^2 s_{\rm r}}\left(2-Ac^3-Bc\right)X(t)^2\\ &+\dot{s}(t)\left\{d^2 s_{\rm r}^2||w||_{L_2}^2 + \frac{c^2}{\beta^2}X(t)^2\right\}.\end{aligned} \tag{126}$$

where $A = \frac{2^9\sqrt{2}s_{\rm r}^6(1+s_{\rm r})(\varepsilon_1-\varepsilon_2)^2}{3\alpha^3(1+\varepsilon_1)^2(1+\varepsilon_2)}$, $B = \frac{16\sqrt{2}s_{\rm r}^2}{\alpha(1+\varepsilon_2)}$. Let c_2 be a positive root of $Ac_2^3 + Bc_2 = 1$. Then, for $0 < \forall c < \bar{c}^* := \min\{c_1, c_2\}$, there exists positive constants $\bar{a}$ and $\bar{b}$ which verifies $\dot{V}_\varepsilon \leq -\bar{b}V_\varepsilon + \bar{a}\dot{s}(t)V_\varepsilon$, which concludes Theorem 6. ■

D. Observer and output feedback control design

With respect to the boundary temperature control introduced in Section VII instead of the heat control, the observer design is replaced by the following.

Corollary 2. *Consider the plant* (102)–(105)*, measurements* $Y_1(t) = s(t)$, $Y_2(t) = T_x(s(t),t)$, *and the following observer*

$$\hat{T}_t(x,t) = \alpha\hat{T}_{xx}(x,t) + p_2(x,Y_1(t))\left(Y_2(t) - \hat{T}_x(Y_1(t),t)\right), \tag{127}$$

$$\hat{T}(0,t) = T_{\rm c}(t) + T_{\rm m}, \tag{128}$$

$$\hat{T}(Y_1(t),t) = T_{\rm m}, \tag{129}$$

where $x \in [0, Y_1(t)]$*, and the observer gain* $p_2(x, Y_1(t))$ *is*

$$p_2(x,Y_1(t)) = -\lambda x \frac{I_1\left(\sqrt{\frac{\lambda}{\alpha}\left(Y_1(t)^2 - x^2\right)}\right)}{\sqrt{\frac{\lambda}{\alpha}\left(Y_1(t)^2-x^2\right)}} \tag{130}$$

with an observer gain $\lambda > 0$*. Assume that the two physical constraints* (106) *and* (34) *are satisfied. Then, for all* $\lambda > 0$*, the observer error system has a unique classical solution and is exponentially stable in the sense of the norm* (62)*.*

The corresponding output feedback controller is designed using the state observer (127)–(130).

Corollary 3. *Consider the closed-loop system consisting of the plant* (102)–(105)*, the measurements* $Y_1(t) = s(t)$ *and* $Y_2(t) = T_x(s(t),t)$*, the observer* (127)–(129)*, and the output feedback control law*

$$T_{\rm c}(t) = -c\left(\frac{1}{\alpha}\int_0^{Y_1(t)} x\left(\hat{T}(x,t) - T_{\rm m}\right)dx + \frac{1}{\beta}Y_1(t)\left(Y_1(t) - s_{\rm r}\right)\right). \tag{131}$$

With c, $\hat{T}_0(x)$, λ *satisfying* (113), (84)*, and* (85)*, respectively, and* $s_{\rm r}$ *satisfying* $s_{\rm r} > s_0 + \frac{\beta s_0^2}{6\alpha}\hat{H}_u$*, the closed-loop system is exponentially stable in the sense of the norm* (87)*.*

The proof of Corollary 2 and Corollary 3 can be established by following the methodology presented in Section V-B and Section VI, respectively.

VIII. Robin Boundary Actuation

Instead of a Neumann or Dirichlet boundary actuation, some physical models require a Robin boundary actuation. For instance, in metal additive manufacturing processes known as Selective Laser Melting [8], the convective heat transfer yields the following energy balance

$$-kT_x(0,t) = -\gamma\left(T(0,t) - T_{\rm a}\right) + I_{\rm c}(t), \tag{132}$$

at the boundary where a laser beam is applied. Here, γ is a heat transfer coefficient, $T_{\rm a}$ is an ambient temperature, and $I_{\rm c}(t)$ is an energy flux induced by the controlled laser beam intensity. For a Robin boundary actuation, the following lemma is stated.

Lemma 7. *If there is a unique classical solution to* (102),(132),(104),(105)*, then for any* $I_{\rm c}(t) > \gamma\left(T(0,t) - T_{\rm a}\right)$ *on the finite time interval* $(0, \bar{t})$*, the condition* (8) *holds.*

Hence, the following condition is required to hold

$$I_{\rm c}(t) > \gamma\left(T(0,t) - T_{\rm a}\right), \quad \forall t > 0. \tag{133}$$

We present the following theorem.

Theorem 7. *Consider a closed-loop system of the plant* (102),(132),(104),(105) *and the control law*

$$I_{\rm c}(t) = -c\left(\frac{k}{\alpha}\int_0^{s(t)}\left(T(x,t) - T_{\rm m}\right)dx + \frac{k}{\beta}\left(s(t) - s_{\rm r}\right)\right) + \gamma\left(T(0,t) - T_{\rm a}\right), \tag{134}$$

where $c > 0$ *is the controller gain, under Assumption 1. Then, for any reference setpoint* $s_{\rm r}$ *satisfying* $s_{\rm r} > s_0 + \frac{\beta}{\alpha}\int_0^{s_0}(T_0(x) - T_{\rm m})dx$*, the closed-loop system is exponentially stable in the sense of the norm* (19)*.*

The proof of Theorem 7 is straightforwardly derived following the methodology employed in Section IV.

IX. Numerical Simulation

For the Stefan problem subject to the Neumann boundary actuation (see Part I), simulation results are performed considering a strip of zinc as in [26]. The physical properties

TABLE I: Physical properties of zinc

Description	Symbol	Value
Density	ρ	$6570\ \mathrm{kg}\cdot\mathrm{m}^{-3}$
Latent heat of fusion	ΔH^*	$111{,}961\mathrm{J}\cdot\mathrm{kg}^{-1}$
Heat Capacity	C_{p}	$389.5687\ \mathrm{J}\cdot\mathrm{kg}^{-1}\cdot\mathrm{K}^{-1}$
Thermal conductivity	k	$116\ \mathrm{w}\cdot\mathrm{m}^{-1}$

of the material are given in Table 1. Consistent simulations to illustrate the feasibility of the backstepping controller with Dirichlet or Robin boundary actuation are easily achievable but due to space limitation, these are not provided. Here, we use the well-known boundary immobilization method combined with finite difference semi-discretization [23]. The initial values are set to s_0 = 0.01 m, and $T_0(x) - T_{\mathrm{m}} = \bar{T}(1 - x/s_0)$ with $\bar{T}$ = 100 K, and the setpoint is chosen as s_{r} = 0.35 m which satisfies the setpoint restriction (15).

A. State feedback control and its robustness

1) Comparison of the pulse input and the backstepping control law: Fig. 4 shows the responses of the plant (45)–(48) with the open-loop pulse input (17) (dashed line) and the backstepping control law (18) (solid line). The time window of the open-loop pulse input is set to 50 min. The gain of the backstepping control law is chosen sufficiently small, c=0.001, to avoid numerical instabilities. Fig. 4 (a) shows the response of $s(t)$ without the parameters perturbations, i.e. $(\varepsilon_1, \varepsilon_2) = (0, 0)$ and clearly demonstrates that $s(t)$ converges to s_{r} applying both rectangular pulse input and backstepping control law. However, the convergence speed is faster with the backstepping control. Moreover, from the dynamics of $s(t)$ under parameters' perturbations $(\varepsilon_1, \varepsilon_2) = (0.3, -0.2)$ shown in Fig. 4 (b), it can be seen that the convergence of $s(t)$ to s_{r} is only achieved with the backstepping control law. On both Fig. 4 (a) and Fig. 4 (b), the responses with the backstepping control law show that the interface position converges faster without the overshoot beyond the setpoint, i.e., $\dot{s}(t) > 0$ and $s_0 < s(t) < s_{\mathrm{r}}$, $\forall t > 0$.

2) Closed-loop system's validity with respect to the physical constraints: The dynamics of the controller $q_{\mathrm{c}}(t)$ and the temperature at the initial interface $T(s_0, t)$ with the backstepping control law (18) are described in Fig. 5 (a) and Fig. 5 (b), respectively, for the system without parameter's uncertainties, i.e., $(\varepsilon_1, \varepsilon_2) = (0, 0)$ (red) and the system with parameters' mismatch $(\varepsilon_1, \varepsilon_2) = (0.3, -0.2)$ (blue). As presented in Fig. 5 (a), the boundary heat controller $q_{\mathrm{c}}(t)$ remains positive, i.e. $q_{\mathrm{c}}(t) > 0$ in both cases. Moreover, Fig. 5 (b) shows that $T(s_0, t)$ converges to T_{m} with $T(s_0, t) > T_{\mathrm{m}}$ for the system with accurate parameters and the system with uncertainties on the parameters. Physically, Fig. 5 (b) means that the temperature at the initial interface's location increases away above the melting temperature T_{m}, which enables the melting of the solid-phase to the setpoint s_{r}. After this significant transient dynamics, $T(s_0, t)$ settles back to T_{m}. An identical behavior is observed when the system is subject to parameters' uncertainty. Therefore, the numerical results are consistent with our theoretical result.

B. Observer design and output feedback control

The initial estimation of the temperature profile is set to $\hat{T}_0(x) - T_{\mathrm{m}} = \bar{\hat{T}}(1 - x/s_0)$ with $\bar{\hat{T}}$ = 10 K while the initial temperature is set to $\bar{T}$ = 1 K, and the observer gain is chosen as λ = 0.001. Then, the restriction on $\hat{T}_0(x)$, λ, and s_{r} described in (84)–(86) are satisfied.

The dynamics of the moving interface $s(t)$, the output feedback controller $q_{\mathrm{c}}(t)$, and the temperature at the initial interface $T(s_0, t)$ are depicted in Fig. 6 (a)–Fig. 6 (c), respectively. Fig. 6 (a) shows that the interface $s(t)$ converges to the setpoint s_{r} without overshoot which is guaranteed in Proposition 2. Fig. 6 (b) shows that the output feedback controller remains positive, which is a physical constraint for the model to be valid as stated in Lemma 1 and ensured in Proposition 2. The model validity can be seen in Fig. 6 (c) which illustrates $T(s_0, t)$ increases from the melting temperature T_{m} to enable melting of material and settles back to its equilibrium. The positivity of the backstepping controller shown in Fig. 6 (b), results from the negativity of the estimation error of the distributed temperature, $\tilde{T}(x, t)$, as shown in Lemma 4 and Proposition 2. Fig. 6 (d) shows the dynamics of estimation errors of temperature profile at $x = 0$ (red), $x = s(t)/4$ (blue), and $x = s(t)/2$ (green), respectively. It is remarkable that the estimation errors at each point converge to zero and remains negative, which confirms the theoretical results stated in Lemma 4 and Proposition 2.

X. CONCLUSION

This paper presented a control and estimation design for the one-phase Stefan problem via backstepping method. The system is described by a diffusion PDE defined on a time-varying spatial domain governed by an ODE.

The novelties of this paper are summarized below.

1) A new approach to globally stabilizing a class of nonlinear parabolic PDEs with moving boundary via a nonlinear backstepping transformation is proposed.
2) The closed-loop responses satisfy the physical constraints needed for the validity of the model.
3) A novel formulation of the Lyapunov function for moving boundary PDEs was applied and it showed the exponential stability of the closed loop system.

Even though our state feedback controller for the Neumann boundary actuation is same as the one proposed in [32], we ensure the exponential stability of the interface and temperature in $\mathcal{H}_1$ norm, which is stronger than the asymptotical stability presented in [32]. The extension of the robustness analysis to the observer-based output feedback is our future work. Note that this hasn't been proved even for coupled diffusion PDE-ODE systems defined on a fixed domain [18]. The application of extremum seeking control with static maps to the Stefan problem following the recent results of [28] could be an interesting design that can be applied to the optimization of phase-change phenomena in building use [24].

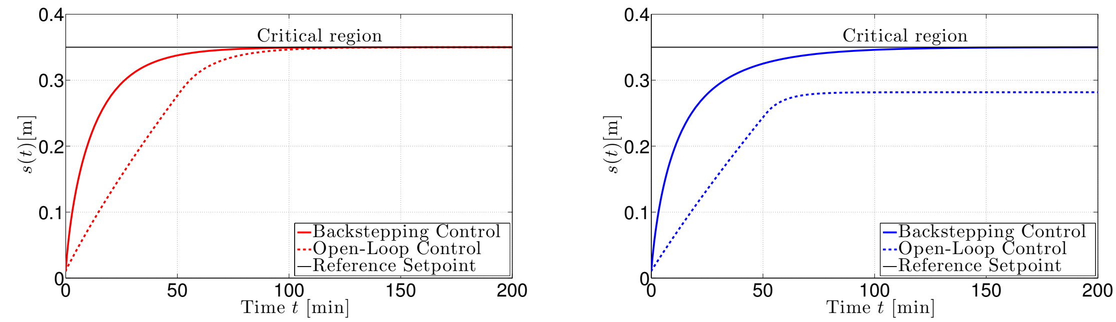

(a) with accurate parameters $(\epsilon_1, \epsilon_2) = (0, 0)$

(b) under parameters perturbation $(\epsilon_1, \epsilon_2) = (0.3, -0.2)$

Fig. 4: The moving interface responses of the plant (45)–(48) with the open-loop pulse input (17) (dashed line) and the backstepping control law (18) (solid line).

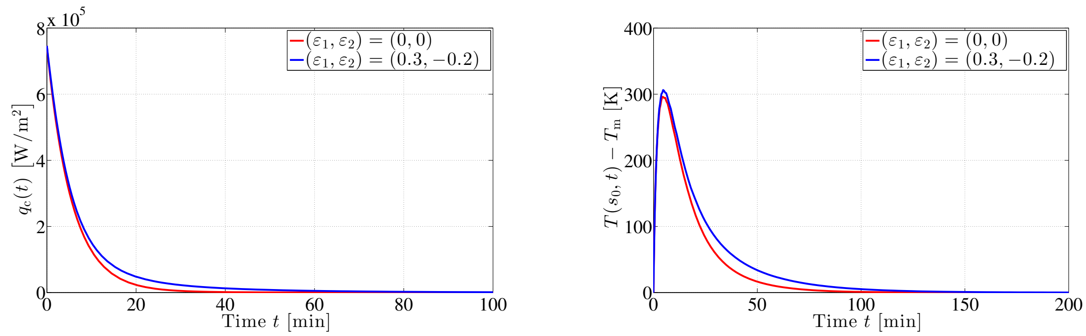

(a) Positivity of the controller remains, i.e. $q_c(t) > 0$.

(b) $T(s_0, t)$ warms up from T_m and returns to it.

Fig. 5: The closed-loop responses of the plant (45)–(48) and the backstepping control law (18) with accurate parameters (red) and parameters perturbation (blue).

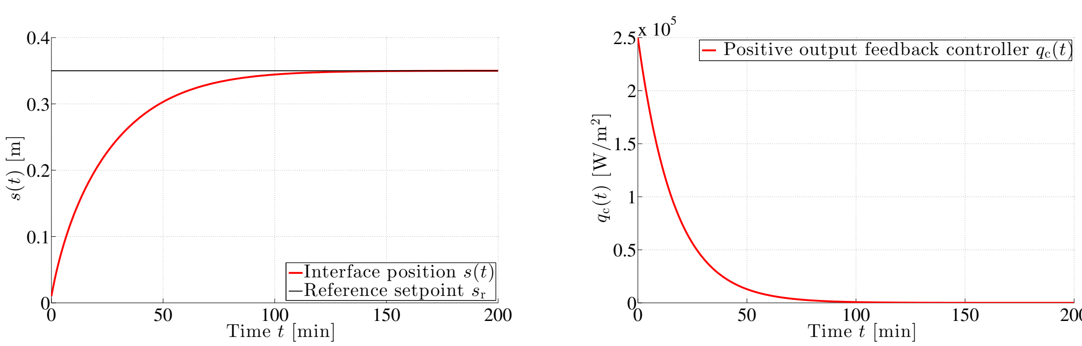

(a) $s(t)$ converges to s_r without overshoot.

(b) Positivity of the output feedback controller remains.

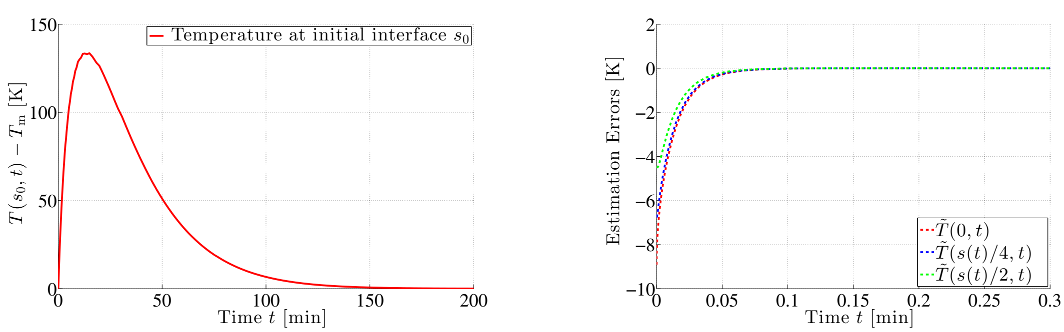

(c) $T(s_0, t)$ warms up from T_m and returns to it.

(d) Negativity of the estimation errors remains.

Fig. 6: Simulation of the closed-loop system (3) - (7) and the estimator (58) - (61) with the output feedback control law (83).

APPENDIX A
THE WELL-POSEDNESS OF THE CLASSICAL SOLUTION OF THE STEFAN PROBLEM

In this section, we define the classical solution of the Stefan problem and state the well-posedness referring to [12].

Definition 1. Under Assumption 1, a pair $(T(x,t), s(t))$ is the classical solution of the one-phase Stefan problem (3)–(7) with $q_{\rm c}(t) \geq 0$ and for all $t < \sigma$, where $0 < \sigma \leq \infty$ if
(i) T_{xx} and T_t are continuous for $0 < x < s(t)$, $0 < t < \sigma$;
(ii) T and T_x are continuous for $0 \leq x \leq s(t)$, $0 < t < \sigma$;
(iii) T is also continuous for $t = 0$, $0 < x \leq s_0$ and $0 \leq \liminf T(x,t) \leq \limsup T(x,t) < \infty$ as $t \to 0$, $x \to 0$;
(iv) $s(t)$ is continuously differentiable for $0 \leq t < \sigma$;
(v) the equations (3)–(7) are satisfied.

Lemma 8. *Assume that $q_{\rm c}(t)$ and $T_0(x)$ are continuously differentiable functions for $\forall t > 0$ and $\forall x \in [0, s_0]$. Then there exists a unique classical solution $(T(x,t), s(t))$ of the system* (3)–(7) *with $q_{\rm c}(t) \geq 0$ and Assumption 1 for all $t > 0$.*

Definition 1 and Lemma 8 hold for a Dirichlet boundary actuation if (106) holds, and for Robin boundary actuation if (133) holds, respectively. Furthermore, both Definition 1 and Lemma 8 can be extended to the generalized parabolic PDE

$$T_t = \alpha(x,t)T_{xx} + b(x,t)T_x + h(x,t)T, \tag{135}$$

provided that $h(x,t) \leq 0$ and the functions α_x, α_{xx}, α_t, b, b_x, and h are Hölder continuous for $0 \leq x < \infty$, $t \geq 0$.

APPENDIX B
BACKSTEPPING TRANSFORMATION FOR MOVING BOUNDARY

1) Direct transformation: Define the general backstepping transformation

$$\begin{aligned} w(x,t) =& u(x,t) - \int_x^{s(t)} k(x-y)u(y,t)dy \\ &- \phi(x - s(t))X(t), \end{aligned} \tag{136}$$

which transforms the reference error system (21)–(24) into the following target system

$$w_t(x,t) = \alpha w_{xx}(x,t) + \dot{s}(t)\phi'(x-s(t))X(t), \tag{137}$$
$$w_x(0,t) = 0, \tag{138}$$
$$w(s(t),t) = 0, \tag{139}$$
$$\dot{X}(t) = -cX(t) - \beta w_x(s(t),t). \tag{140}$$

The stability of the target system (137)–(140) is guaranteed if $\dot{s}(t) > 0$, $s_0 < s(t) < s_{\rm r}$ as shown in Appendix C-1. Then, taking first and second spatial derivatives of (136) and the first time derivative of (136), we obtain the following relation

$$\begin{aligned} w_t(x,t) -& \alpha w_{xx}(x,t) - \dot{s}(t)\phi'(x-s(t))X(t) \\ =& -(\alpha k(x-s(t)) - \beta\phi(x-s(t)))u_x(s(t),t) \\ &+ \alpha\phi''(x-s(t))X(t). \end{aligned} \tag{141}$$

Evaluating (136) and its spatial derivative at $x = s(t)$, we have

$$w(s(t),t) = -\phi(0)X(t), \tag{142}$$
$$w_x(s(t),t) = u_x(s(t),t) - \phi'(0)X(t). \tag{143}$$

In order to map (21)–(24) into (137)–(140) for any continuous functions $(u(x,t), X(t))$ through the transformation (141)–(143), the kernel functions $k(x-y)$ and $\phi(x)$ must satisfy

$$\phi''(x-s(t)) = 0, \quad \phi(0) = 0, \quad \phi'(0) = \frac{c}{\beta}, \tag{144}$$
$$k(x-y) = \frac{\beta}{\alpha}\phi(x-y). \tag{145}$$

From (144), the solution to the gain kernel is given by (26).

2) Inverse transformation: Suppose that the inverse transformation that maps (137)–(140) into (21)–(24) writes

$$\begin{aligned} u(x,t) =& w(x,t) + \int_x^{s(t)} l(x-y)w(y,t)dy \\ &+ \psi(x-s(t))X(t), \end{aligned} \tag{146}$$

where $l(x-y)$, $\psi(x-s(t))$ are the kernel functions. Taking derivative of (146) with respect to t and x, respectively, along the solution of (27)–(30), the following relations are derived

$$\begin{aligned} &u_t(x,t) - \alpha u_{xx}(x,t) \\ &= \left\{ \frac{c}{\beta}\left(1 + \int_x^{s(t)} l(x-y)dy\right) - \psi'(x-s(t)) \right\} \dot{s}(t)X(t) \\ &+ (\alpha l(x-s(t)) - \beta\psi(x-s(t)))\, w_x(s(t),t) \\ &- (c\psi(x-s(t)) + \alpha\psi''(x-s(t)))\, X(t). \end{aligned} \tag{147}$$

$$u(s(t),t) = \psi(0)X(t), \tag{148}$$
$$u_x(s(t),t) = w_x(s(t),t) + \psi'(0)X(t). \tag{149}$$

From (148)–(147), one can deduce that in order to recover the original system(21)–(24) for any continuous functions $(w(x,t), X(t))$, $\psi(x)$ and $l(x-y)$ must satisfy

$$\psi''(x) = -\frac{c}{\alpha}\psi(x), \quad \psi(0) = 0, \quad \psi'(0) = \frac{c}{\beta}, \tag{150}$$
$$l(x-s(t)) = \frac{\beta}{\alpha}\psi(x-s(t)), \tag{151}$$
$$\psi'(x-s(t)) = \frac{c}{\beta}\left(1 + \int_x^{s(t)} l(x-y)dy\right). \tag{152}$$

The solution to (150) is given by (32), from which $l(x-y)$ can be deduced using (151). These solutions satisfy the condition (152) as well.

APPENDIX C
STABILITY ANALYSIS

In this section, we prove the exponential stability of (w, X) system defined in (137)–(140) via Lyapunov analysis, which induces the stability of the original (u, X) system. The following assumptions on the interface dynamics

$$\dot{s}(t) > 0, \quad 0 < s_0 < s(t) < s_{\rm r}, \tag{153}$$

which are shown in Section IV-B are stated.

1) Stability of the target system: Firstly, we show the exponential stability of the target system (137)–(140). Consider the Lyapunov function V such that

$$V = \frac{1}{2}||w||_{\mathcal{H}_1}^2 + \frac{p}{2}X(t)^2, \tag{154}$$

with a positive number $p > 0$ to be chosen later. Then, noting that the boundary condition (139) yields $w_t(s(t),t) = -\dot{s}(t)w_x(s(t),t)$, by chain rule $\frac{d}{dt}w(s(t),t) = w_t(s(t),t) + \dot{s}(t)w_x(s(t),t) = 0$, the time derivative of (154) along the solution of the target system (137)–(140) yields

$$\begin{aligned}\dot{V} =& -\alpha||w_{xx}||_{L_2}^2 - \alpha||w_x||_{L_2}^2 \\ & - pcX(t)^2 - p\beta X(t)w_x(s(t),t) \\ & + \dot{s}(t)\left(-\phi'(0)X(t)w_x(s(t),t) - \frac{1}{2}w_x(s(t),t)^2\right) \\ & + \dot{s}(t)X(t)\left(\phi''(s(t))w(0,t)\right. \\ & \left. + \int_0^{s(t)} f(x-s(t))w(x,t)dx\right),\end{aligned} \tag{155}$$

where $f(x) = \phi'(x) - \phi'''(x)$. Define $m = \int_0^{s_{\rm r}} f(-x)^2dx$. Using (153), Young's, Cauchy Schwarz, Poincare's, Agmon's inequality, and choosing $p = \frac{c\alpha}{4\beta^2 s_{\rm r}}$, we have

$$\begin{aligned}\dot{V} \leq& -\frac{\alpha}{2}||w_{xx}||_{L_2}^2 - \alpha||w_x||_{L_2}^2 \\ & - \frac{pc}{2}X(t)^2 + \dot{s}(t)\left\{\frac{1+\phi'(0)^2}{2}X(t)^2\right. \\ & \left. + 4s_{\rm r}\phi''(s(t))^2||w_x||_{L_2}^2 + m||w||_{L_2}^2\right\}, \\ \leq& -\frac{\alpha}{8s_{\rm r}^2}||w||_{\mathcal{H}_1}^2 - \frac{pc}{2}X(t)^2 + \dot{s}(t)\left\{4s_{\rm r}\overline{\phi''}||w_x||_{L_2}^2\right. \\ & \left. + m||w||_{L_2}^2 + \frac{1+\phi'(0)^2}{2}X(t)^2\right\}, \\ \leq& -bV + a\dot{s}(t)V,\end{aligned} \tag{156}$$

where $a = 2\max\left\{4s_{\rm r}\overline{\phi''}, m, \frac{1+\phi'(0)^2}{2p}\right\}$, $b = \min\left\{\frac{\alpha}{4s_{\rm r}^2}, c\right\}$, and $\overline{\phi''} := \sup_{0\leq s(t)\leq s_{\rm r}} \phi''(s(t))^2$.

2) Exponential stability for the original (u, X)-system: The norm equivalence between the target system and original system is shown using the direct and the inverse transformation, (136) and (146), respectively. Taking the square of (146) and applying Young's and Cauchy Schwarz inequality, we have

$$\begin{aligned}u(x,t)^2 \leq& 3\psi(x-s(t))^2X(t)^2 + 3w(x,t)^2 \\ & + \frac{3\beta^2}{\alpha^2}\left(\int_x^{s(t)}\psi(x-y)^2dy\right)\left(\int_x^{s(t)}w(y,t)^2dy\right).\end{aligned} \tag{157}$$

Integrating (157) on $[0, s(t)]$ and applying Cauchy Schwarz inequality with the help of (153), we have $||u||_{L_2}^2 \leq 3\left(1 + \frac{\beta^2 s_{\rm r} N_1}{\alpha^2}\right)||w||_{L_2}^2 + 3N_1X(t)^2$, where $N_1 := \int_0^{s_{\rm r}}\psi(-x)^2dx$. Similarly, taking the spatial derivative of (146), we have $||u_x||_{L_2}^2 \leq 3||w_x||_{L_2}^2 + 3\frac{\beta^2}{\alpha^2}\left(\psi(0)^2 + s_{\rm r}N_2\right)||w||_{L_2}^2 + 3N_2X(t)^2$, where $N_2 := \int_0^{s_{\rm r}}\psi'(-x)^2dx$. Since $\phi(0) = \psi(0) = 0$, the following estimates hold:

$$||w||_{L_2}^2 \leq M_1||u||_{L_2}^2 + M_2X(t)^2, \tag{158}$$

$$||w_x||_{L_2}^2 \leq 3||u_x||_{L_2}^2 + M_3||u||_{L_2}^2 + M_4X(t)^2, \tag{159}$$

$$||u||_{L_2}^2 \leq M_5||w||_{L_2}^2 + M_6X(t)^2, \tag{160}$$

$$||u_x||_{L_2}^2 \leq 3||w_x||_{L_2}^2 + M_7||w||_{L_2}^2 + M_8X(t)^2, \tag{161}$$

where $M_1 = 3\left(1 + \frac{\beta^2}{\alpha^2}s_{\rm r}\left(\int_0^{s_{\rm r}}\phi(-x)^2dx\right)\right)$, $M_2 = 3\left(\int_0^{s_{\rm r}}\phi(-x)^2dx\right)$, $M_3 = 3\frac{\beta^2}{\alpha^2}s_{\rm r}\left(\int_0^{s_{\rm r}}\phi'(-x)^2dx\right)$, $M_4 = 3\left(\int_0^{s_{\rm r}}\phi'(-x)^2dx\right)$, $M_5 = 3\left(1 + \frac{\beta^2}{\alpha^2}s_{\rm r}N_1\right)$, $M_6 = 3N_1$, $M_7 = 3\frac{\beta^2}{\alpha^2}s_{\rm r}N_2$, $M_8 = 3N_2$. Adding (158) to (159) and (160) to (161), we derive the following inequality

$$\begin{aligned}\underline{\delta}\left(||u||_{\mathcal{H}_1}^2 + X(t)^2\right) \leq& ||w||_{\mathcal{H}_1}^2 + pX(t)^2 \\ \leq& \bar{\delta}\left(||u||_{\mathcal{H}_1}^2 + X(t)^2\right),\end{aligned} \tag{162}$$

where $\bar{\delta} = \max\{M_1 + M_3, p + M_2 + M_4\}$, $\underline{\delta} = \frac{\min\{1,p\}}{\max\{M_5+M_7, M_6+M_8+1\}}$. Define a parameter $D > 0$ as $D = \frac{\bar{\delta}}{\underline{\delta}}e^{as_{\rm r}}$. Then, with the help of (162), (43), we deduce that there exists $D > 0$ and $b > 0$ such that

$$||u||_{\mathcal{H}_1}^2 + X(t)^2 \leq D\left(||u_0||_{\mathcal{H}_1}^2 + X(0)^2\right)e^{-bt}. \tag{163}$$

Acknowledgment

The authors would like to thank S. Tang for her help to ensure the first result of Theorem 1.

References

[1] A. Armaou and P.D. Christofides, "Robust control of parabolic PDE systems with time-dependent spatial domains," *Automatica*, vol. 37, pp. 61–69, 2001.

[2] N. Bekiaris-Liberis and M. Krstic, "Compensation of state-dependent input delay for nonlinear systems," *IEEE Transactions on Automatic Control*, vol. 58, no. 2, pp. 275–289, Feb. 2013.

[3] N. Bekiaris-Liberis and M. Krstic, "Compensation of wave actuator dynamics for nonlinear systems," *IEEE Transactions on Automatic Control*, vol. 59(6), pp.1555-1570, 2014.

[4] N. Boonkumkrong and S. Kuntanapreeda, "Backstepping boundary control: An application to rod temperature control with Neumann boundary condition," *Proceedings of the Institution of Mechanical Engineers, Part I: Journal of Systems and Control Engineering*, vol. 228(5), pp.295-302, 2014.

[5] D. M. Boskovic, M. Krstic, and W. Liu, "Boundary control of an unstable heat equation via measurement of domain-averaged temperature," *IEEE Transactions on Automatic Control*, vol. 46(12), pp. 2022–2028, 2001.

[6] X. Cai and M. Krstic, "Nonlinear control under wave actuator dynamics with time- and state-dependent moving boundary," *International Journal of Robust and Nonlinear Control*, vol. 25(2), pp.222-251, 2015.

[7] P.D. Christofides, "Robust control of parabolic PDE systems," *Chemical Engineering Science*, vol. 53, pp. 2949–2965, 1998.

[8] H. Chung and S. Das, "Numerical modeling of scanning laser-induced melting, vaporization and resolidification in metals subjected to step heat flux input," *International journal of heat and mass transfer*, vol. 47(19), pp.4153-4164, 2004.

[9] F. Conrad, D. Hilhorst, and T.I. Seidman, "Well-posedness of a moving boundary problem arising in a dissolution-growth process," *Nonlinear Analysis*, vol. 15, pp. 445–465, 1990.

[10] N. Daraoui, P. Dufour, H. Hammouri, and A. Hottot, "Model predictive control during the primary drying stage of lyophilisation," *Control Engineering Practice*, vol. 18, pp. 483–494, 2010.

[11] M. Diagne, N. Bekiaris-Liberis, A. Otto, and M. Krstic, "Control of Transport PDE/Nonlinear ODE Cascades with State-Dependent Propagation Speed," *IEEE Transactions on Automatic Control*, vol. 62, no. 12, pp. 6278-6293, 2017.

[12] A. Friedman "Free boundary problems for parabolic equations I. Melting of solids," Journal of Mathematics and Mechanics, vol. 8(4), pp.499-517, 1959.

[13] A. Friedman and F. Reitich, "Analysis of a mathematical model for the growth of tumors," *Journal of mathematical biology*, vol. 38(3), pp.262-284, 1999.
[14] S. Gupta, *The Classical Stefan Problem. Basic Concepts, Modelling and Analysis*. North-Holland: Applied mathematics and Mechanics, 2003.
[15] M. Izadi and S. Dubljevic, "Backstepping output feedback control of moving boundary parabolic PDEs," *European Journal of Control*, vol. 21, pp. 27 – 35, 2015.
[16] S. Koga, M. Diagne, S. Tang, and M. Krstic, "Backstepping control of the one-phase Stefan problem," In *2016 American Control Conference (ACC)*, pages 2548–2553. IEEE, 2016.
[17] S. Koga, M. Diagne, and M. Krstic, "Output feedback control of the one-phase Stefan problem," In *55th Conference on Decision and Control (CDC)*, pages 526–531. IEEE, 2016.
[18] M. Krstic, "Compensating actuator and sensor dynamics governed by diffusion PDEs," *Systems & Control Letters*, vol. 58, pp. 372–377, 2009.
[19] M. Krstic, "Input delay compensation for forward complete and strict-feedforward nonlinear systems," *IEEE Transactions on Automatic Control*, vol. 55(2), pp.287-303, 2010.
[20] M. Krstic and A. Smyshlyaev, "Backstepping boundary control for first-order hyperbolic PDEs and application to systems with actuator and sensor delays," *Systems & Control Letters*, vol. 57, pp. 750–758, 2008.
[21] M. Krstic and A. Smyshlyaev, *Boundary Control of PDEs: A Course on Backstepping Designs*. Singapore: SIAM, 2008.
[22] M. Krstic and A. Smyshlyaev, " Adaptive boundary control for unstable parabolic PDEs–Part I: Lyapunov Design," *IEEE Transactions on Automatic Control*, vol. 53(7), pp. 1575–1591, 2008.
[23] S. Kutluay, A. R. Bahadir, and A. Özdes, "The numerical solution of one-phase classical Stefan problem," *Journal of computational and applied mathematics*, 81.1, pp. 135-144, 1997.
[24] F. Kuznik, J. Virgone, and J. Noel, "Optimization of a phase change material wallboard for building use," *Applied Thermal Engineering*, vol. 28(11), pp.1291-1298, 2008.
[25] C. Lei, Z. Lin, and H. Wang, "The free boundary problem describing information diffusion in online social networks," *Journal of Differential Equations*, vol. 254(3), pp.1326-1341, 2013.
[26] A. Maidi and J.-P. Corriou, "Boundary geometric control of a linear stefan problem," *Journal of Process Control*, vol. 24, pp. 939–946, 2014.
[27] G.A. Maykut and N. Untersteiner, "Some results from a time dependent thermodynamic model of sea ice," *Journal of Geophysical Research*, vol. 76, pp. 1550–1575, 1971.
[28] T.R. Oliveira, M. Krstic, and D. Tsubakino, "Extremum seeking for static maps with delays," *IEEE Transactions on Automatic Control*, vol. 62(4), pp.1911-1926, 2017.
[29] C.V. Pao, *Nonlinear Parabolic and Elliptic Equations*. Springer, 1992.
[30] N. Petit, "Control problems for one-dimensional fluids and reactive fluids with moving interfaces," In *Advances in the theory of control, signals and systems with physical modeling*, volume 407 of *Lecture notes in control and information sciences*, pages 323–337, Lausanne, Dec 2010.
[31] B. Petrus, J. Bentsman, and B.G. Thomas, "Enthalpy-based feedback control algorithms for the Stefan problem," *Decision and Control (CDC), 2012 IEEE 51st Annual Conference on*, pp. 7037–7042, 2012.
[32] B. Petrus, J. Bentsman, and B.G. Thomas, "Feedback control of the two-phase Stefan problem, with an application to the continuous casting of steel," *Decision and Control (CDC), 2010 49th IEEE Conference on*, pp. 1731–1736, 2010.
[33] A. Smyshlyaev and M. Krstic, "Closed-form boundary state feedbacks for a class of 1-D partial integro-differential equations," *IEEE Transactions on Automatic Control*, vol. 49(12), pp. 2185–2202, 2004.
[34] A. Smyshlyaev and M. Krstic, " Backstepping observers for a class of parabolic PDEs," *Systems & Control Letters*, vol. 54(7), pp. 613–625, 2005.
[35] A. Smyshlyaev and M. Krstic, "On control design for PDEs with space-dependent diffusivity or time-dependent reactivity," *Automatica*, vol. 41(9), pp. 1601–1608, 2005.
[36] A. Smyshlyaev and M. Krstic, "Adaptive boundary control for unstable parabolic PDEs–Part II: Estimation-based designs," *Automatica*, vol. 43(9), pp. 1543–1556, 2007.
[37] A. Smyshlyaev and M. Krstic, "Adaptive boundary control for unstable parabolic PDEs–Part III: Output feedback examples with swapping identifiers," *Automatica*, vol. 43(9), pp. 1557–1564, 2007.
[38] V. Srinivasan and J. Newman, "Discharge model for the lithium iron-phosphate electrode," *Journal of the Electrochemical Society*, vol. 151, pp. A1517–A1529, 2004.
[39] J. Stefan, "Uber die Theorie der Eisbildung, insbesondere uber die Eisbildung im Polarmeere," *Annalen der Physik*, vol. 278, pp. 269–286, 1891.
[40] G.A. Susto and M. Krstic, "Control of PDE–ODE cascades with Neumann interconnections," *Journal of the Franklin Institute*, vol. 347, pp. 284–314, 2010.
[41] S. Tang and C. Xie, "State and output feedback boundary control for a coupled PDE–ODE system," *Systems & Control Letters*, vol. 60, pp. 540–545, 2011.
[42] J.S. Wettlaufer, "Heat flux at the ice-ocean interface," *Journal of Geophysical Research: Oceans*, vol. 96, pp. 7215–7236, 1991.
[43] B. Zalba, J.M. Marin, L.F. Cabeza, and H. Mehling, "Review on thermal energy storage with phase change: materials, heat transfer analysis and applications," *Applied thermal engineering*, vol. 23, pp. 251–283, 2003.

Shumon Koga received the B.S. degree in applied physics from Keio University (Japan), and the M.S. degree in mechanical and aerospace engineering from the University of California, San Diego (USA). He is currently pursuing the Ph.D. degree in mechanical and aerospace engineering at the University of California, San Diego. His research interests include the control of distributed parameter systems, free boundary problem, and thermodynamical system.

Mamadou Diagne received his Ph.D. degree in 2013 at Laboratoire d'Automatique et du Génie des Procédés, Université Claude Bernard Lyon I. He has been a postdoctoral fellow at the Cymer Center for Control Systems and Dynamics of University of California San Diego from 2013 to 2015 and at the Department of Mechanical Engineering of the University of Michigan from 2015 to 2016. He is currently an Assistant Professor at Rensselaer Polytechnic Institute. His research interests concern the modeling and the control of heat and mass transport phenomena, production/manufacturing systems and additive manufacturing processes described by partial differential equations and delay systems.

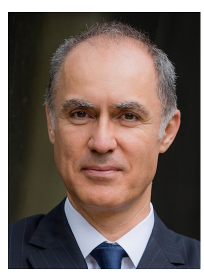

Miroslav Krstic (S'92-M'95-SM'99-F'02) holds the Alspach endowed chair and is the founding director of the Cymer Center for Control Systems and Dynamics at UC San Diego. He also serves as Associate Vice Chancellor for Research at UCSD. As a graduate student, Krstic won the UC Santa Barbara best dissertation award and student best paper awards at CDC and ACC. Krstic is Fellow of IEEE, IFAC, ASME, SIAM, and IET (UK), Associate Fellow of AIAA, and foreign member of the Academy of Engineering of Serbia. He has received the PECASE, NSF Career, and ONR Young Investigator awards, the Axelby and Schuck paper prizes, the Chestnut textbook prize, the ASME Nyquist Lecture Prize, and the first UCSD Research Award given to an engineer. Krstic has also been awarded the Springer Visiting Professorship at UC Berkeley, the Distinguished Visiting Fellowship of the Royal Academy of Engineering, the Invitation Fellowship of the Japan Society for the Promotion of Science, and the Honorary Professorships from the Northeastern University (Shenyang) and the Chongqing University, China. He serves as Senior Editor in IEEE Transactions on Automatic Control and Automatica, as editor of two Springer book series, and has served as Vice President for Technical Activities of the IEEE Control Systems Society and as chair of the IEEE CSS Fellow Committee. Krstic has coauthored eleven books on adaptive, nonlinear, and stochastic control, extremum seeking, control of PDE systems including turbulent flows, and control of delay systems.